Carbohydrate Polymers 112 (2014) 235–244

Contents lists available at ScienceDirect

Carbohydrate Polymers

journal homepage: www.elsevier.com/locate/carbpol

Alginate based hybrid copolymer hydrogels—Influence of pore morphology on cell–material interaction

Finosh Gnanaprakasam Thankam, Jayabalan Muthu *

Sree ChitraTirunal Institute for Medical Sciences and Technology, Polymer Science Division, BMT Wing, Poojapura, Thiruvananthapuram 695 012, Kerala, India

ARTICLE INFO

Article history:
Received 17 March 2014
Received in revised form 16 May 2014
Accepted 19 May 2014
Available online 6 June 2014

Keywords:
Alginate hybrid copolymer
Morphologically modified hydrogels
Physical properties
Cell–material interaction

ABSTRACT

Alginate based hybrid copolymer hydrogels with unidirectional pore morphology were prepared to achieve synergistic biological performance for cardiac tissue engineering applications. Alginate based hybrid copolymer (ALGP) were prepared using alginate and poly(propylene fumarate) (HT-PPF) units. Different hybrid bimodal hydrogels were prepared by covalent crosslinking using poly(ethylene glycol diacrylate) and vinyl monomer viz acrylic acid, methyl methacrylate, butyl methacrylate and *N*-*N*′-methylene-bis-acrylamide and ionic crosslinking with calcium. The morphologically modified hydrogels (MM-hydrogels) with unidirectional elongated pores and high aspect ratio were prepared. MM-hydrogels favour better mechanical properties; it also enhances cell viability and infiltration due to unidirectional pores. However, the crosslinkers influence the fibroblast infiltration of these hydrogels. Synthesis of collagen and fibroblast infiltration was greater for alginate copolymer crosslinked with poly(ethylene glycol diacrylate–acrylic acid (ALGP–PA) even after one month (288%). This hybrid MM-hydrogel promoted cardiomyoblast growth on to their interstices signifying its potent applications in cardiac tissue engineering.

1. Introduction

Hydrogels form an ideal choice for tissue engineering owing to their close resemblance with native extracellular matrix (ECM), inherent cellular interactions, biocompatibility, water holding capacity and fantabulous biological performance. The porosity in hydrogels permits local angiogenesis and fluid flux which is very crucial for neo-organogenesis (Gerecht et al., 2007). With hydrogels intended for tissue engineering applications, inter connecting pores contributes mostly to the maintenance of viability of the cells seeded on to it. The porosity also aid in channelling and trafficking the nutrients and the metabolic wastes in the form of solutes and gases to and from the growing cells even in the absence of functional blood capillaries. It also promotes vasculature formation, cell penetration and communication (Elbert, 2011; Rao, Sasaki, & Taguchi, 2013). The porosity determines the stability of the hydrogel in biological fluids. The porosity and pore size relates inversely with the stability and directly with the degradation of the hydrogels (Dahlin, Kasper, & Mikos, 2011). The porosity of a hydrogel favours tissue formation and function by guiding the cells towards inner networks by a process called contact guidance (Provenzano, Inman, Eliceiri, Trier, & Keely, 2008). The porosity is also essential for cell distribution and interconnection (Khademhosseini & Langer, 2007).

The magnitude of synthesis of extra cellular matrix (ECM) on the hydrogel is also influenced by the porosity and pore size (Lien, Ko, & Huang, 2009). The pores of the hydrogels can contribute to the mechanical interlocking *in vivo* with the surrounding native tissues and biomolecules thereby enhance the stability at the interface (Kock, van Donkelaar, & Ito, 2012). The maximum thickness for a viable hydrogel, which lacks a functional capillary network for tissue genesis, was reported to be around 150–200 μm. In addition, beyond this limit the seeded cells fail to survive due to insufficient oxygen diffusion and nutrient transport towards the inner rooms of the hydrogel (Fidkowski et al., 2005). The requirement for porosity may vary with respect to cell type, size and function. The optimum pore size required for the initiation of vascularization is around 5 μm and for fibroblast ingrowths to be 5–15 μm (Whang et al., 1999). For the growth of cardiomyocytes, 50 μm size pores are sufficient (Barry et al., 2005).

The success of the tissue engineering hydrogels depends not only on the cell growth but also on the uniform distribution of the cells on it. For proper contact guidance, these hydrogels should possess oriented morphologies that will direct the cells towards

* Corresponding author. Tel.: +91 471 2520212; fax: +91 471 234814.
E-mail addresses: mjayabalan52@gmail.com, alan@sctimst.ac.in, jaybalan@sctimst.ac.in (J. Muthu).

http://dx.doi.org/10.1016/j.carbpol.2014.05.083
0144-8617/

the pore direction. The micro sized pores can promote the proliferation and cell migration (Schulte et al., 2013). However, the pore size should be uniform and optimal. If the pore size is too small, the cells cannot migrate and form a confluent layer. If too large, the ligands for cell attachment will be diluted which may affect the cell spreading. The most commonly used technique for the preparation of porous hydrogel is solvent casting/particulate leaching and freeze-drying (Quirk, France, Shakesheff, & Howdle, 2004; Thomson, Wake, Yaszemski, & Mikos, 1995). However, these techniques have inadequacies to have a control over the pore orientation and interconnectivity (Quirk et al., 2004; Ho et al., 2004). Even though the porosity plays a significant role in cell–material interaction, the orientation of the pore architecture of hydrogels to a particular direction can enhance the biological responses due to the effective channelling of metabolites and wastes.

As a hydrogel and scaffold material, alginate gained importance for tissue engineering and cell delivery systems, especially for cardiac applications (Andersen, Strand, Formo, Alsberg, & Christensen, 2011). The tissue engineering scaffolds based on the synthetic poly ester, poly(propylene fumarate) (PPF) has been proven to be biocompatible and support cell growth (Muthu, Shalumon, & Mitha, 2009). However, a synergistic biological performance of a hybrid hydrogel of alginate and PPF is always desirable. Based on this background we introduced unidirectional pore orientation and interconnectivity in alginate based hybrid hydrogels by controlled stretching in water-swollen hydrogels. Alginate based morphologically modified hydrogels (MM-hydrogels) were prepared using hybrid copolymer of alginate and PPF and vinyl crosslinkers. The performances of these hydrogels with unidirectional elongated pore morphology and high aspect ratio were found to be greater when compared with that of normal ones. The present article deals with the salient features of the MM-hydrogels and its influence on the biological performance with emphasis on tissue engineering.

2. Materials and methods

2.1. Materials

Sodium alginate (guluronic acid (39%) and mannuronic acid (61%) from brown algae, medium viscosity, product no. A2033), maleic anhydride, acrylic acid (AA), *N*-*N*′-methylene-bis-acrylamide (NMBA), methyl methacrylate (MMA), poly(ethylene glycol diacrylate) (PEGDA), calcium chloride, L-ascorbic acid, ammonium per sulfate, etc. were obtained from Sigma Aldrich, Spruce Street, St. Louis, USA. Sodium acetate and sodium hydroxide were supplied by Merck specialties Pvt. Ltd, Mumbai, India. *N*-Butyl methacrylate (BMA) was purchased from Polyscience Inc., Warrington. 1,2-Propylene glycol and morpholine were provided by SD fine chemicals India Ltd.

2.2. Preparation of alginate based hybrid copolymer hydrogels

Alginate based hybrid copolymer hydrogels were prepared by using sodium alginate and poly(propylene fumarate) (HT-PPF). Hydroxyl terminated-poly(propylene fumarate) (HT-PPF) was synthesized by the condensation polymerization of maleic anhydride with 1,2-propylene glycol as per our published method (Mitha & Muthu, 2009). Briefly, the reactants were refluxed in presence of catalysts (sodium acetate and morpholine) at 145 °C for 2 h. The temperature was raised to 185 °C vacuum condensation was conducted. HT-PPF so formed was purified using acetone–methanol and stored at room temperature for further studies. HT-PPF was warmed at 70–80 °C under acidic condition and double volume of Na-alginate powder was immediately added under stirring condition, mixed well and allowed to set for more than 30 min. The entire mixture was then slowly dissolved in minimum volume of distilled water under constant stirring to form alginate–PPF (ALGP) copolymer resin.

The hybrid hydrogel were prepared by a bimodal crosslinking followed by solvent casting and freeze-drying. The bimodal crosslinking was introduced with covalent and ionic crosslinking of fumarate and alginates units, respectively. The fumarate double bonds of the PPF in the ALGP were crosslinked with PEGDA with residual free double bonds of PEGDA crosslinked with other vinyl monomers viz. AA, BMA, MMA and NMBA. Initially pre-hydrogel sheet was prepared by blending ALGP copolymer resin with PEGDA at 70 °C in presence of water and casting at 60 °C. The pre-hydrogel sheet so formed after casting was then treated with 10% $CaCl_2$ solution for 4 h and then with ascorbic acid/ammonium persulphate solution for 1 h to form solid fully crosslinked hydrogel. The hydrogel scaffold was then freeze-dried. This is coded as ALGP-P. The formulation is given in Table 1. Similarly, four more hybrid hydrogel were prepared by blending ALGP copolymer resin with the combination of PEGDA and vinyl monomer viz. ALGP copolymer resin/PEGDA/AA, ALGP copolymer resin/PEGDA/BMA, ALGP copolymer resin/PEGDA/MMA, and ALGP copolymer resin/PEGDA/NMBA. These hydrogels are coded as ALGP-PA, ALGP-PB, ALGP-PM and ALGP-PN, respectively. The hydrogels were stored aseptically for further evaluations.

2.3. Preparation of ALGP based morphologically modified hydrogels (MM-hydrogels)

Prior to the morphological modification of the hydrogels, the number of cycles of cyclic stretching completed before rupture (fatigue life cycles) was determined. The instrument employed was dynamic mechanical tester (M/S Test Recourses, USA). The water-swollen hydrogel samples (1.5 cm × 4 cm) were fixed to the instrument, connected to a liquid chamber filled with distilled water at 37 °C. The samples were subjected to cyclic stretching under tensile mode using a load of 0.91 N with a frequency of 6 cycles/s and amplitude of 2.5 mm. The numbers of cycles of cyclic stretching completed before rupture (fatigue life) were recorded by MTL-Windows-v7.1 software supplied with the instrument until the rupture of the hydrogel samples. The MM-hydrogels with unidirectional elongated pores and high aspect ratio were prepared by subjecting the as prepared hydrogel to cyclic stretching to one fourth of the complete fatigue life. These MM-hydrogel were then cleaned, freeze-dried and sterilized using ethylene oxide and used for further evaluations.

2.4. Characterizations of hydrogels

The physicochemical and thermal properties of the MM-hydrogels were evaluated as per our published method (Gnanaprakasam Thankam & Muthu, 2013a; Gnanaprakasam Thankam, Muthu, Sankar, & Kozhiparambil Gopal, 2013). AT-IR spectra were recorded by using Nicolet 5700 FTIR Spectrometer. The surface hydrophilicity of the hydrogels was evaluated by measuring contact angle measured using KSV Sigma tensiometer (KSV Instruments Ltd, USA). Both advancing and receding contact angles were determined. The swelling (%) (S) and equilibrium water content (EWC) of the hydrogels were determined under dry and wet condition using the following equations as reported in our previous work (Gnanaprakasam Thankam & Muthu, 2013b).

$$\mathrm{EWC} = \frac{\text{wet weight} - \text{dry weight}}{\text{wet weight}} \times 100$$

$$S = \frac{\text{wet weight}}{\text{wet weight}} \times 100$$

Table 1
Formulation of alginate based hybrid copolymer hydrogels.

Reactants	Concentration of reactants in hydrogels (wt%)				
	ALGP-P	ALGP-PA	ALGP-PB	ALGP-PM	ALGP-PN
ALGP copolymer resin	89	94.5	89	89	91.5
Polyethylene glycol diacrylate	11	2.75	5.5	5.5	5.75
Acrylic acid	–	2.75	–	–	–
n-Butyl methacrylate	–	–	5.5	–	–
Methyl methacrylate	–	–	–	5.5	–
N-*N*′-Methylene-bis-acrylamide	–	–	–	–	2.75

The thermal transition state of water in the hydrogels was investigated by differential scanning calorimetry (DSC) as per our published method (Gnanaprakasam Thankam & Muthu, 2013b). A DSC-2920 (M/S TA Instruments Inc. USA) was used. The hydrogel samples (around 20 mg) were cooled to (−)70 °C and then heated to 100 °C. Both the heating and cooling processes were monitored. All the hydrogel samples were tested before and after stretching. From the enthalpy of melting (obtained from DSC thermogram) and EWC, the status of the water (freezing free water, freezing bound water and non-freezing bound water) present in the hydrogels was assessed. The status of the water in the hydrogels before and after stretching was then compared.

The changes in surface and pore morphology induced by controlled unidirectional stretching of the hydrogels were investigated by ESEM analysis (FEI, Quanta-200, USA). The hydrogels were shock-frozen in liquid nitrogen for 1 min to fracture the sample without any external force. The cross section of the fractured sample was analyzed by scanning electron microscopy at low vacuum mode. Twenty pores were randomly taken from the surface portion and cross section from each image for analysis. The images taken (by focusing the edges of the hydrogels to see the interior pore architecture) were compared with that of as prepared samples using the imaging software ImageJ 1.46r and multi-measure plugin. The pore length (longest dimension of pore) and the pore width (shortest dimension of pore) of the hydrogel scaffolds were measured. The ratio of pore length to width gives the pore aspect ratio.

2.5. Determination of cell viability by direct contact assay and live/dead assay on hydrogels

The viability of fibroblast cells grown on MM-hydrogels was monitored by live/dead assay using acridine orange/ethidium bromide cocktail after 5 days of initial seeding. L929 fibroblast cell lines (NCCS, Pune) were used. The toxicity imparted by the hydrogels on contact with L929 cells were monitored by direct contact assay (Gnanaprakasam Thankam & Muthu, 2013a).

2.6. Determination of collagen deposition in hydrogels

The deposition of collagen in MM-hydrogels by L929 fibroblast cells was investigated. The amount of collagen adsorbed on the ALGP hydrogel scaffolds before and after stretching, was determined by Sirius red method. The L929 fibroblast cells were grown on the hydrogels for 10 days. Then the collagen deposited on the hydrogels was stained with Sirius red, excess stain was washed with diluted HCl, dye stained collagen was solubilized in NaOH and the absorbance was measured at 530 nm. A control without scaffolds and a blank without cells were also maintained in the similar manner. From the OD values the percentage variation in collagen was calculated (Vandrovcová et al., 2011).

2.7. Determination of fibroblast proliferation and long-term viability by MTT assay

The percentage of fibroblasts adhered on to the surface and proliferated to the inner pores of all the ALGP hydrogels were determined by a modified MTT assay for a period of one month as reported elsewhere (Gnanaprakasam Thankam et al., 2013). The percentage viability of the cells grown and proliferated inside the hydrogels was calculated.

2.8. Growth of H9c2 cardiomyoblasts on MM-hydrogels

The attachment and proliferation of H9c2 cardiomyoblast cells was investigated for five days as per previously published protocols using fluorescein diacetate (FDA) (Yokoyama, Danjo, Ogawa, & Wakabayashi, 1997). The cardiomyoblast-grown hydrogels were washed with PBS and stained with FDA (100 μg/ml). After 10 min incubation in dark, the cells were imaged on fluorescent microscope using blue filter (M/S Optika SRL, Italy).

2.9. Statistical analysis

All experiments consisted of 5 or 6 samples from each group. The values are presented as means ± standard deviations. Statistical analysis was done with one way ANOVA using online calculator, Statistics Calculator version-3 beta and the level of significance was set at $P < 0.05$ for all calculations.

3. Results and discussions

3.1. Preparation of alginate based hybrid hydrogels

Synthetic biodegradable polymers are apt for tissue engineering applications due to reproducible and controllable chemical characteristics, degradable linkages, and crosslinking abilities. The similarities with native extra cellular matrix (ECM) make the naturally derived polymers a better choice for tissue engineering applications (Drury & Mooney, 2003). Most often, the synthetic scaffolds are inadequate in providing the biological responses for cell growth and tissue genesis (Almany & Seliktar, 2005). On the other hand, the natural polymers like alginate are less adaptable when considering the mechanical properties and degradation rate (Li & Guan, 2011). By using hybrid copolymer of synthetic and natural polymers, it is possible to minimize the major drawbacks individual application of these polysaccharides. We were able to enhance the physiochemical and mechanical properties as well as the biological responses of alginate hydrogels by combining it with HT-PPF.

Alginate based hybrid hydrogels were synthesized using alginate–PPF hybrid copolymer resin (ALGP). Alginate–PPF hybrid copolymer resin (ALGP) was prepared by condensation reaction involving free —COOH group from the manuronic segment of Na-alginate and the terminal —OH group of HT-PPF. Alginate

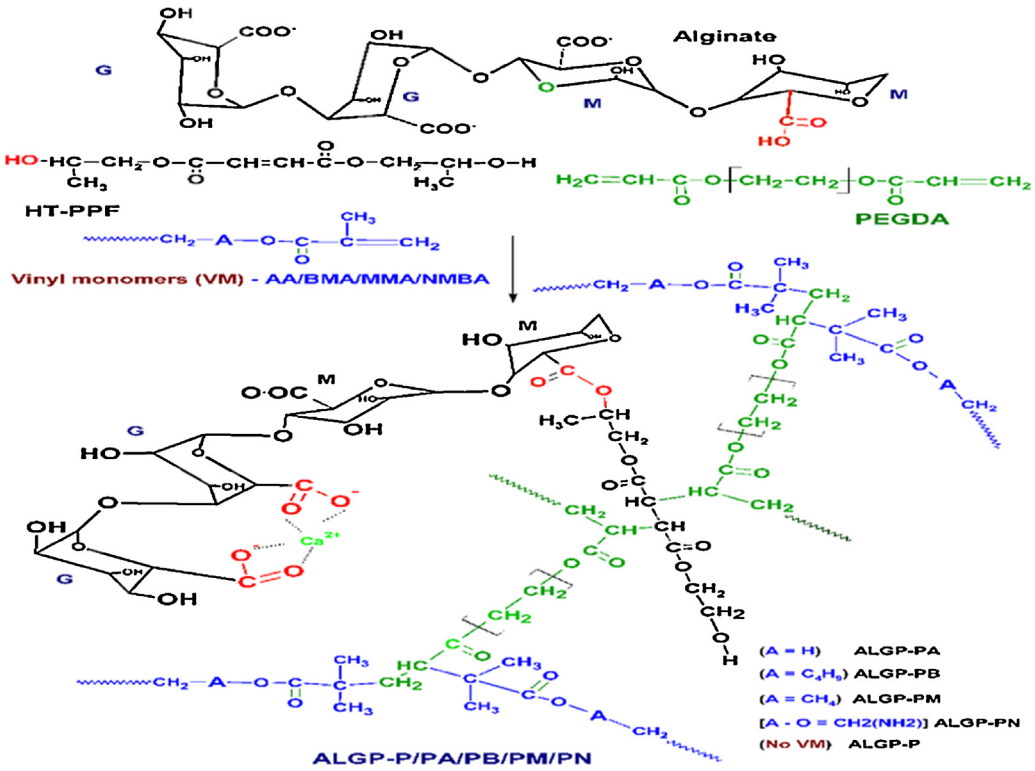

Fig. 1. Synthesis of biosynthetic ALGP copolymer and crosslinking reaction schemes for the preparation of hydrogels.

based hybrid hydrogels were prepared by two-step crosslinking reactions. In the first step of crosslinking, the double bonds present in the fumaric acid fraction of the ALGP copolymer was crosslinked by PEGDA and the residual double bonds with vinyl monomer (acrylic acid/BMA/MMA/NMBA) to form partially crosslinked hybrid hydrogels. In the second step crosslinking, the alginate fraction of all the partially crosslinked hydrogels were crosslinked with Ca^{2+} to form fully crosslinked hydrogels. The hydrogels prepared with vinyl monomers, acrylic acid, BMA, MMA and NMBA are coded as ALGP-PA, ALGP-PB, ALGP-PM and ALGP-PN, respectively. The reaction scheme for the synthesis and crosslinking reaction of alginate–PPF hybrid copolymer resin involved in the preparing of hydrogels are given in Fig. 1

3.2. Preparation of MM-hydrogels with unidirectional pores

The number of cycles of cyclic stretching (fatigue life) tolerated by the as prepared hybrid hydrogels was determined under accelerated conditions in water at physiological temperature. The results are given in Table 2. ALGP-PA hydrogel withstood greater number of stretching cycles. ALGP-P and ALGP-PM showed an intermediate value. The hydrophilicity imparted by the acrylic acid on ALGP-PA hydrogel, the consequent water uptake and hydrogen bonding imparts flexibility to withstand more number of flexing before breaking. ALGP-PB and ALGP-PN exhibited lesser number of cycles, which may be due to the rigidity induced by the hydrophobic BMA by excluding much of the free and bulk water in the former and the rigidity imparted by extensive crosslinking by the two double bonds of NMBA in the latter. The unidirectional pores are formed in the present hydrogel during the cyclic stretching limited to 1/4th cycles of the complete fatigue life of each hydrogels. These MM-hydrogels were freeze-dried.

3.3. Characterization of MM-hydrogels

3.3.1. ATR-IR analyses of MM-hydrogels

The ATR-IR spectra (Fig. 2) of the MM-hydrogels revealed a broad peak around 3200–3500 cm^{-1} for the presence of —OH groups on the surface of the hydrogel. The peaks around 2900 cm^{-1} are due to the asymmetric stretching of —CH— groups. The peak around 1700 cm^{-1} revealed the carbonyl stretching of HT-PPF segments which indicates ester formation. The peaks around 1600 cm^{-1} and 1400 cm^{-1} are due to the asymmetric and symmetric stretching for —COOH groups in the hydrogel surface. These peaks (1600 cm^{-1} and 1400 cm^{-1}) are also due to the asymmetric

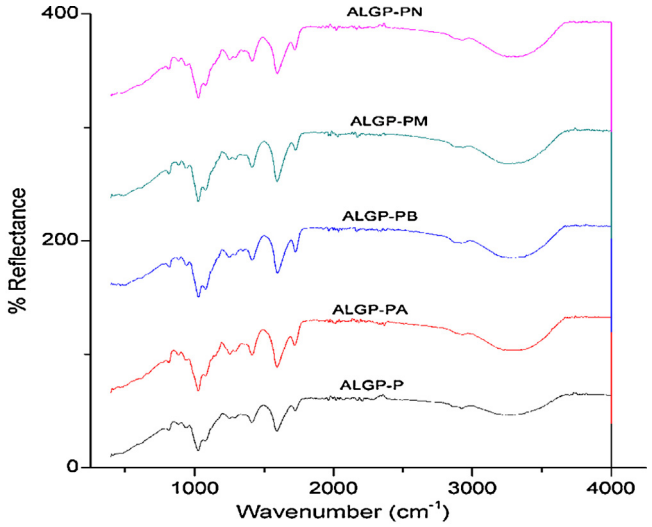

Fig. 2. IR spectrum of ALGP based MM-hydrogels.

Table 2
Properties of alginate based hybrid copolymer hydrogels after unidirectional stretching.

Analyses	Parameters ($n=6$)	Alginate based hybrid copolymer hydrogels				
		ALGP-P	ALGP-PA	ALGP-PB	ALGP-PM	ALGP-PN
Fatigue life	No. of cycles	>30,000	>70,000	>3000	>26,000	>8000
Surface	Advancing contact angle (°)	44.06 ± 6.89	43.42 ± 2.42	50.23 ± 5.2	40.97 ± 4.53	42.77 ± 5.49
	Receding contact angle (°)	40.89 ± 4.69	43.7 ± 2.39	50.32 ± 6.21	41.64 ± 4.3	43.55 ± 5.64
DSC analyses of water	Onset of melting temp. of freezing water (°C)	−0.60	−0.55	−0.28	−0.37	−0.53
	Enthalpy of melting of freezing water (J/g)	162	166.2	64.2	125.5	93.47
Swelling and EWC	Swelling (%) ($P<0.01$)	264.4 ± 37.33	165.60 ± 0.21	77.49 ± 3	202.16 ± 8.89	137.7 ± 9.58
	EWC ($P<0.001$)	72.33 ± 3.05	62.35 ± 0.03	43.65 ± 0.95	66.88 ± 0.98	57.77 ± 1.52

and symmetric stretching vibrations of C=C stretching of unsaturated fumarate groups of HT-PPF segment. The peaks around 1200 cm^{-1} and 1028 cm^{-1} are due to the asymmetric and symmetric stretch of —C—O—C— of alginate. The ATR-IR analyses confirmed the hybrid copolymer formation and effective crosslinking.

3.3.2. Pore morphology in hydrogels

Pore size and porosity of the hydrogel scaffolds are significant factors, which strongly influence the cell ingrowths (Guo et al., 2013). The large pore volume enhances the cell attachment and accommodates greater cell mass by effectively trafficking the nutrients and metabolites. This will also pave way to neovascularization that is very essential for tissue formation. The pore size for the scaffold for a particular application depends on the type and diameter of cells used. The average pore size required by various cells range from 5 μm to 500 μm (Yang, Leong, Du, & Chua, 2001). The mass transport and cell migration depends on the pore interconnectivity of scaffolds. *In vivo*, the cells residing around 200 μm away from the blood circulation are highly susceptible for apoptotic or necrotic death due to low oxygen tension and insufficient nutrient availability (Colton, 1995). In the case of tissue engineering hydrogels, this issue can be overcome by the inherent porosity and pore interconnectivity present in the biodegradable hydrogels (Cohen, Yoshioka, Lucarelli, Hwang, & Langer, 1991). Such pores can effectively channel the metabolites and exhausts to and from the surviving cells. Nevertheless, there are chances for the closure of small pores by the invasion of fibrous tissue and nonspecific protein adsorption during the initial stages of cell seeding. Still the pore size, morphology and orientation determine the cell infiltration (Bauer, 1975). The unidirectional pores and pore interconnectivity imparted by controlled stretching offered a better cell attachment and proliferation on our hydrogel scaffolds.

The surface pore morphology is a reflection of the internal pore architecture of the hydrogels. The ESEM analysis of MM-hydrogels reveals alignment of pores towards the direction of applied stress (Fig. 3). The images displayed an extension in the pore length and/or width, which was quantified by ImageJ software. The aspect ratio reveals considerable increase of pore size for ALGP-PA and ALGP-PM. Though slight increase is observed for ALGP-PB and ALGP-PN, a reverse trend is observed with ALGP-P. This is because of the limited crosslinking interactions in ALGP-P due to the absence of the second vinyl crosslinker, which are present in the other four hydrogels. Still there is an increase in both length and width. ALGP-PA and ALGP-PM showed a decrease in width after stretching that resulted in the increase in the aspect ratio (Table 3).

The major demerits associated with most scaffolds having low pore volume are the limited cell penetration, non-homogeneous cell distribution, low cell viability, time consumption and so on (Chan & Leong, 2008). In such scaffolds, the surface area available for cell adhesion and protein adsorption is very limited. This affects the cellular metabolism (Gnanaprakasam Thankam & Muthu, 2013b). The present controlled cyclic stretching has introduced unidirectional pores, pore opening and pore inter connectivity in ALGP-PA and ALGP-PM hydrogels. The resultant increase in pore aspect ratio and pore volume is favourable for accommodating more cell population. Since the pore aspect ratio is determined using freeze-dried samples, the surface area of the scaffolds may increase further after attaining maximum swelling in the medium that are favouarble for cells proliferation and penetration.

3.3.3. Surface properties of hydrogels

The amphiphilicity offers cell migration, communication, and the effective channelling of biomolecules to and from the surrounding medium (Munoz-Pinto, Hou, Grunlan, Hahn, & Schoener, 2010). The adhesion, migration, and proliferation of different type cells and the adsorption of proteins depend on scaffold surface characteristics, wettability, and hydrophilicity. Marques et al. reported

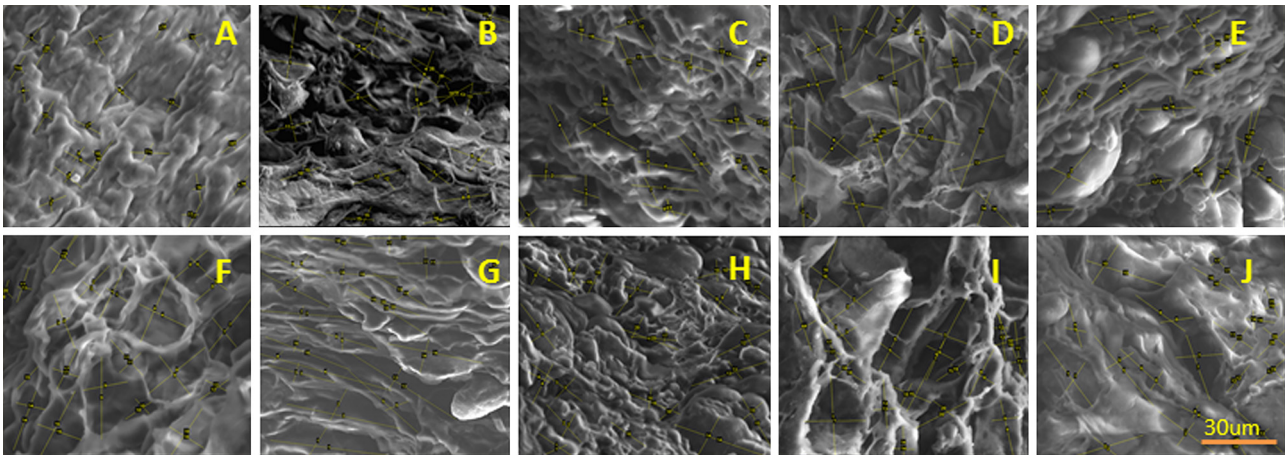

Fig. 3. ESEM analysis of as prepared and MM-hydrogels. ALGP-P, ALGP-PA, ALGP-PB, ALGP-PM and ALGP-PN hydrogels before stretching ((A)–(E)) and after stretching ((F)–(J)), respectively.

Table 3
Pore size analyses of alginate based hybrid copolymer hydrogels.

Hydrogels	As prepared/morphologically modified hydrogel	Pore length (μm)	Pore width (μm)	Aspect ratio
ALGP-P	As prepared	12.07 ± 2.81	6.35 ± 1.62	2.00 ± 0.62
	Morphologically modified	20.59 ± 5.69	12.00 ± 4.18	1.78 ± 0.33
ALGP-PA	As prepared	17.67 ± 3.5	9.43 ± 2.61	1.97 ± 0.49
	Morphologically modified	34.00 ± 8.96	8.93 ± 3.52	4.54 ± 2.50
ALGP-PB	As prepared	17.46 ± 4.43	8.85 ± 2.54	2.06 ± 0.55
	Morphologically modified	21.87 ± 5.13	9.52 ± 2.44	2.38 ± 0.63
ALGP-PM	As prepared	23.25 ± 7.11	13.87 ± 6.18	1.85 ± 0.62
	Morphologically modified	21.68 ± 8.18	9.86 ± 3.07	2.89 ± 0.73
ALGP-PN	As prepared	18.68 ± 4.97	8.54 ± 2.57	2.26 ± 0.63
	Morphologically modified	20.58 ± 7.15	9.62 ± 4.12	2.31 ± 0.68

that amphiphilicity promotes the adsorption of serum proteins via weak and reversible bonds. The protein adsorption enhances cell attachment. Because the cell first interacts with these weakly adsorbed serum proteins before they can secrete their own adhesion proteins onto the hydrogel substratum (Marques, Reis, & Hunt, 2002). All the MM-hydrogel exhibited a surface amphiphilicity as evident from the contact angle values (Table 2). The ALGP-PM is found to be relatively more hydrophilic while ALGP-PB showed lesser hydrophilicity among the five hydrogels. The other three have moderate hydrophilicity.

3.3.4. Swelling, equilibrium water content and freezable water content of hydrogels

The swelling of hydrogel is a function of counter acting osmotic and dispersing forces. The osmotic forces drive the water into the networks, while the dispersing forces exerted by the polymer chains of hydrogel network prevent the incoming water. The dispersing forces depend on crosslinking and hydrophobicity. According to Zhou these swelling events are due to the hydrophilicity of the functional groups and crosslinking efficiency (Zhou & Wu, 2011). Among the MM-hydrogels, the water holding capacity and swelling of ALGP-PB hydrogel is comparatively low (Table 2). This may due to the lesser hydrophilicity of the vinyl cross linker BMA. ALGP-PN also has moderate value, which may be due to the higher crosslinking through NMBA with its two vinyl functional groups.

The process of swelling involves several stages. Initially the water molecules entering the matrix hydrate the polar hydrophilic functional groups. This type of water constitutes the primary bound water. The primary bound water results in the expansion of the hydrogel matrix, thereby increasing its volume and subsequently expose the less polar groups. The hydrophobically bound water can constitute secondary bound water. These waters (primary bound water and secondary bound water) together constitute freezable bound water. During this stage, the crosslinks of the hydrogels resist the osmotic driving force of the water. This can lead to the intake of additional amount of water until an equilibrium swelling is attained. This type of water is the bulk water or free water (Helena Janik, 2010). The free water behaves similarly with pure water and does not form hydrogen bonds with the functional groups in the hydrogel. While the freezable bound water has very weak interaction with the hydrogel matrix, it produces a characteristic shift in freezing and melting temperature when compared with that of pure water. The nonfreezing bound water is the one that forms hydrogen bonds with the hydrogel functional groups and deviates from the normal thermal properties associated with the pure water (Higuchi, Komiyama, & Iijima, 1984).

The nature of water present inside the hydrogel network influences the biomimetic properties like biocompatibility, adsorption of proteins and cellular components, antithrombogenicity, channelling of metabolites etc. The bulk and freezing bound water can remove the hydration shell of the biomolecules, influence the adsorption/desorption of biomolecules and enable the seeded cells to penetrate, proliferate and function (Shoichet, 2010). We have reported the effect of water on the growth and survival of fibroblast and cardiomyoblast cells on the biosynthetic poly vinyl alcohol–alginate hydrogels (Gnanaprakasam Thankam et al., 2013). In the present study, the effect of modified pore morphology on the nature of water is also investigated.

The DSC thermograms of the present hydrogels displayed exothermic peaks corresponding to the crystallization during cooling phase and endothermic peaks for the melting of freezable free and freezable bound water during heating phase (Fig. 4). From the enthalpy of melting and the equilibrium water content of the corresponding hydrogels, the percentage of freezing water and nonfreezing water of the hydrogels can be calculated (Xiang, Zhang, & Chen, 2006). The estimation of freezing and nonfreezing water content of the as prepared hydrogels reveals higher freezing water content only in ALGP-PA. Other as prepared hydrogels have higher nonfreezing water content (Table 4).

The effect of cyclic stretching on the nature of the water in the MM-hydrogels was investigated. The controlled stretching in the MM-hydrogels has considerable influence on the nature of water. The MM-hydrogels of ALGP-P and ALGP-PA possessed around 50% freezable water content while the remaining hydrogels exhibited lesser freezable water content. ALGP-PB had exhibited only 19% freezable water content. However, all the five hydrogels have decreased nonfreezing water content in comparison to the as prepared hydrogels. This may be due to the increase in pore size and aspect ratio imparted by controlled stretching that enabled the entry and occupancy of more water molecules on the voids of the MM-hydrogels. The modified pore morphology with reduced nonfreezable water content can enhance the overall performance of the scaffolds.

Table 4
Nature of water in alginate based hybrid copolymer hydrogels.

Nature of water in the hydrogel	Alginate based hybrid copolymer hydrogels				
	ALGP-P	ALGP-PA	ALGP-PB	ALGP-PM	ALGP-PN
As prepared					
Freezable water content (%)	17.07	50.75	14.19	22.57	29.26
Nonfreezing water content (W_{nf}) (%)	44.05	22.61	64.57	58.74	42.69
Morphologically modified					
Freezable water content (%)	48.5	49.76	19.16	37.43	27.99
Nonfreezing water content (W_{nf}) (%)	23.83	12.59	24.49	29.45	29.78

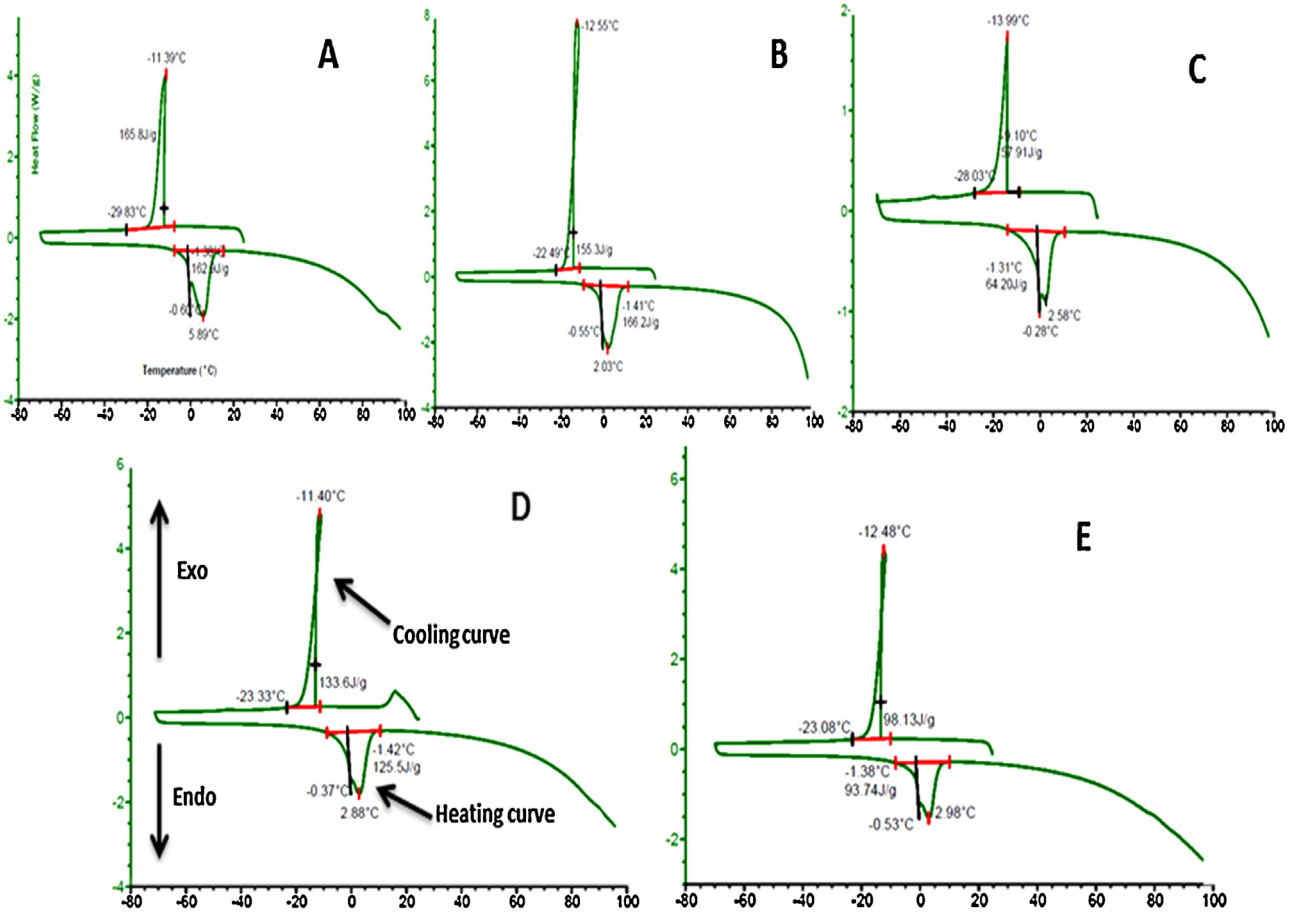

Fig. 4. DSC analysis of MM-hydrogels. ALGP-P (A), ALGP-PA (B), ALGP-PB (C), ALGP-PM (D) and ALGP-PN (E) hydrogels showing characteristic peaks corresponding to the crystallization and melting of freezing water.

3.4. Influence of modified pore morphology in hydrogels on biological responses

The influence of pore morphology and surface imparted by the cyclic stretching has not affected the normal cellular activities. The cytotoxicity evaluations by direct contact assay revealed no characteristic change in cell morphology upon contact of L929 fibroblast cells with the MM-hydrogels (Fig. 5). The cells were found to be proliferating in a normal way beneath the hydrogels. The altered pore morphology introduced by mechanochemical methods and the possible degradation products are nontoxic to the cells. The live dead assay after 5 days of initial seeding also displayed green fluorescence of cells on all the hydrogels revealing the non-apoptotic, healthy and spreading of cells on to the interstices of the hydrogels as reported elsewhere (Gnanaprakasam Thankam et al., 2013; Zeltinger, Sherwood, Graham, Müeller, & Griffith, 2001). The cell density with MM-hydrogel ALGP-PB is relatively low when compared with the other MM-hydrogels. Even though the pore aspect ratio of ALGP-PB hydrogel is increased after stretching, the freezable water content and swelling is lower when compared with other MM-hydrogels. The reduced freezable water content and swelling restricted the availability of nutrients and metabolites to the survival of the cells, which lowered the cell population.

The cells growing on a hydrogel scaffolds secrete and deposit extracellular matrix (ECM) to withstand the mechanical and biological stresses. The extra cellular responses are critical for the long-term viability and functioning of the seeded cells (Stock et al., 2001). Since collagen is the most abundant component of ECM, its quantification offers a clear picture of the total ECM deposition (Cox & Erler, 2011). It has been reported that the porosity has a direct influence on the secretion and deposition of ECM (Mandal and Kundu, 2009). The ECM produced by the cells is deposited in the pores and filled in the voids as the hydrogel degrades. This leads to the generation of a neo tissue (Bryant & Anseth, 2003). The collagen synthesis on the present hydrogels is given in Fig. 6. The results are given as percentage increase in OD with respect to the control. The assay results showed an increase in OD for the MM-hydrogels in comparison to the corresponding as prepared ones. A drastic increase in OD is observed for ALGP-PA hydrogel. This indicates the availability of sufficient space on these hydrogels for accommodating more cells. The stretching of the present hydrogels has increased the void volume and subsequent ECM deposition. This effect was found to be relatively greater in ALGP-PA hydrogel while the other hydrogels also exhibited an appreciable effect.

The cell penetration and three-dimensional growth in hydrogel scaffolds is largely influenced by the pore length of the scaffolds. The cell penetration and three-dimensional growth of L929 fibroblast cells in the present MM-hydrogels during the period of 1 month were quantified. The viability of the cells in the hydrogels increased during the course of time (Fig. 6). The hydrogels ALGP-P, ALGP-PN and ALGP-PM exhibited a viability of around 50% on 10th day; on 30th day, these hydrogels exhibited 100% viability. However, a dramatic increase of 288% viability was observed in the case of ALGP-PA hydrogel. The cell viability with ALGP-PB hydrogel reduced with time after 23 days. Therefore, these results were not included in the figure. The cell percentage viability of the as prepared samples was found to be lower when compared with morphologically modified ones. The L929 fibroblast cells seeded on

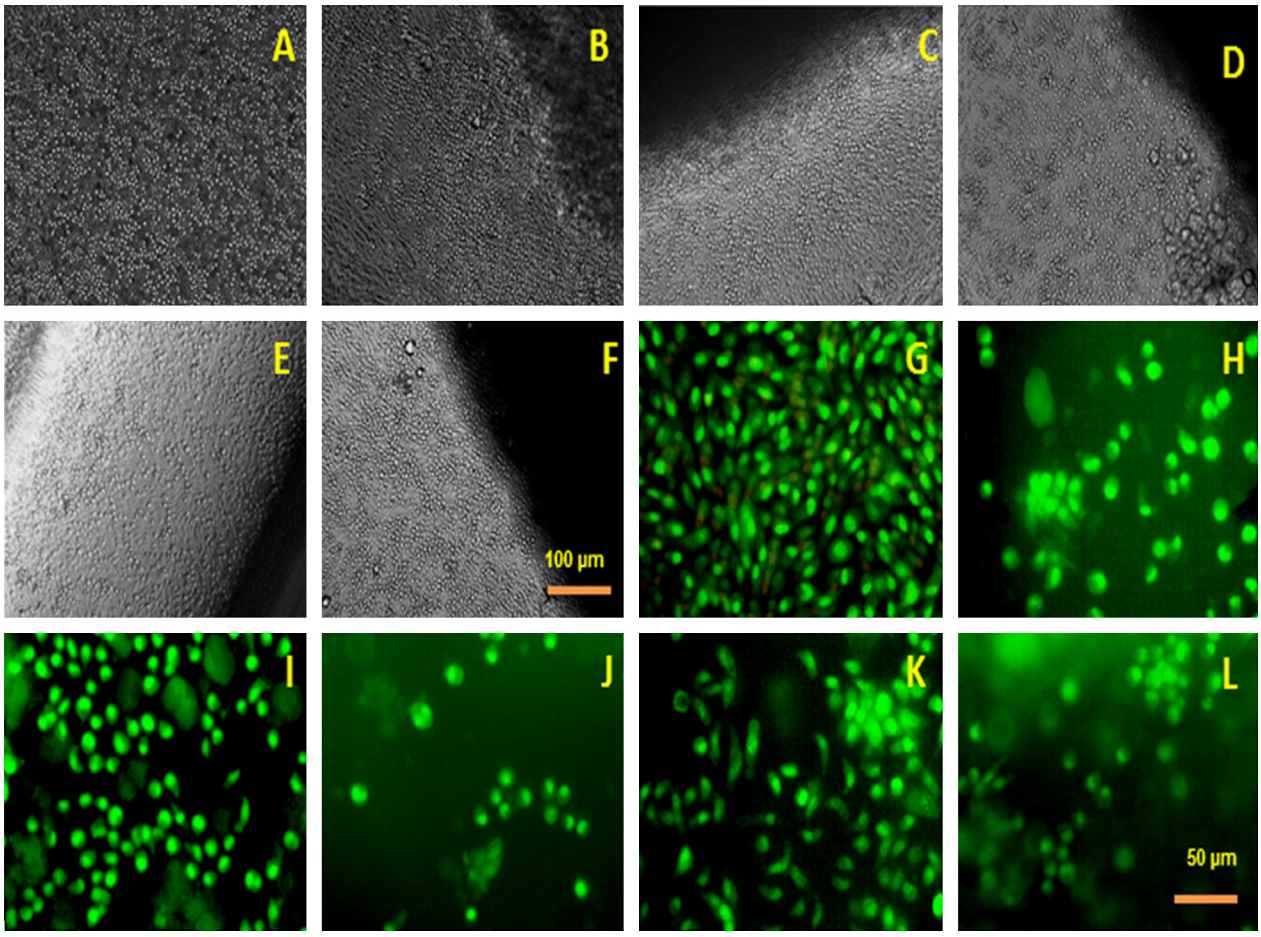

Fig. 5. Cytotoxicity evaluation of MM-hydrogels. Images (A)–(F) for direct contact assay ((A) for control and (B)–(F) for ALGP-P, ALGP-PA, ALGP-PB, ALGP-PM and ALGP-PN hydrogels, respectively) and (G)–(K) for live dead assay ((G) for control and (H)–(K) for ALGP-P, ALGP-PA, ALGP-PB, ALGP-PM and ALGP-PN hydrogels, respectively).

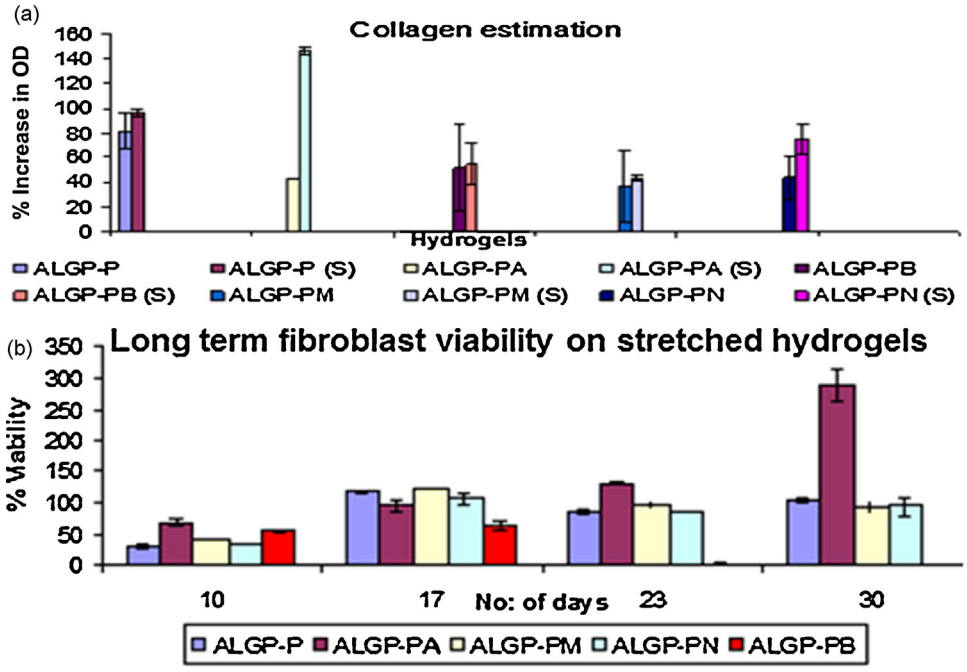

Fig. 6. Deposition of collagen estimation in the as prepared and MM-hydrogels (*S* indicates the stretched samples) (a). Fibroblast proliferation in the MM-hydrogels (b).

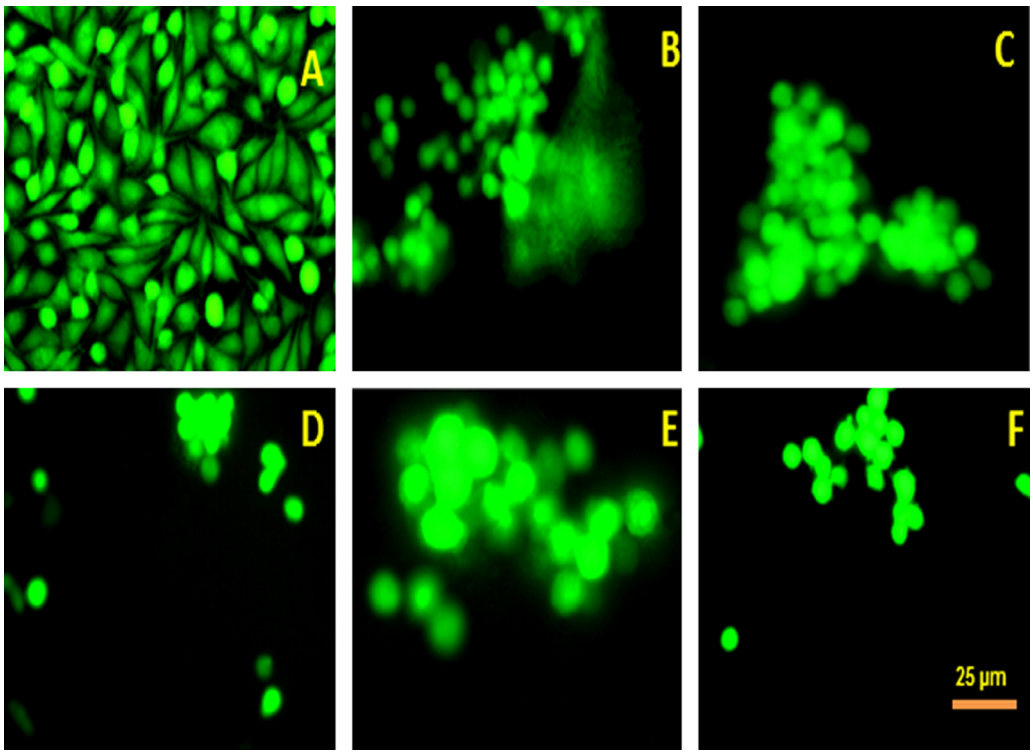

Fig. 7. FDA stained images of H9c2 cells grown on MM-hydrogels ((A) for control and (B)–(F) for ALGP-P, ALGP-PA, ALGP-PB, ALGP-PM and ALGP-PN hydrogels, respectively).

the surface of the scaffolds attach and penetrate into the hydrogel networks that are facilitated by the unidirectional pore orientation and the free water present in the hydrogel networks as reported elsewhere (Ma, Mao, & Gao, 2007). Moreover, these hydrogels are saturated with the nutrients and the growth factors present in the medium. In addition, the stress induced by the population of proliferating cells crowded on the pores force them to enter the unoccupied rooms of the interior network. The penetration depth of cells for the hydrogels were reported to be 200 μm beyond which the cells form a necrotic core if surplus nutrition is not available (Huang et al., 2012). The pore dimensions of the present hydrogels fall within the acceptable limit.

The attachment and proliferation of H9c2 cardiomyoblast cells on MM-hydrogels was assessed. FDA stained images of H9c2 cells grown on MM-hydrogels are given in Fig. 7. With all the MM-hydrogels, H9c2 cells have grown as clusters. The density of the cells in the clusters was found to be greater in ALGP-PA followed by ALGP-PM and ALGP-P. The minimum cell density was obtained for ALGP-PB and ALGP-PN. The studies reveal that L929 and H9c2 cells were able to maintain their viability and function on these bare MM-hydrogels (without any growth factors or signalling molecules).

4. Conclusions

Controlled cyclic stretching of alginate-based hybrid hydrogels could change the morphology of pores with unidirectional and macro-micro interconnected pores with higher aspect ratio. Physiochemical evaluations signify the improved characteristics essential for tissue engineering applications. Cell culture studies on H9c2 and L929 cell lines showed better and favourable cell responses. The improved pore morphology can promote cell penetration and impart long-term viability and function. The remarkable cellular responses (fibroblast and cardiomyoblast viability and infiltration) observed with hybrid MM-hydrogel, ALGP-PA reveal its potential applications in cardiac tissue engineering.

Acknowledgements

Thanks are due to The Director, SCTIMST and Head, BMT Wing, SCTIMST, Thiruvananthapuram-695012 for providing the facilities to carry out this work. G.T.F. acknowledges the financial support from Department of Science & technology, New Delhi, Government of India and KSCST&E, Kerala, India.

References

Almany, L., & Seliktar, D. (2005). Biosynthetic hydrogel scaffolds made from fibrinogen and polyethylene glycol for 3D cell cultures. *Biomaterials*, *26*(15), 2467–2477. http://dx.doi.org/10.1016/j.biomaterials.2004.06.047

Andersen, T., Strand, B. L., Formo, K., Alsberg, E., & Christensen, B. E. (2011). Chapter 9 Alginates as biomaterials in tissue engineering. In *Carbohydrate chemistry*. Retrieved from ⟨http://pubs.rsc.org/en/content/chapter/bk9781849731546-00227/978-1-84973-154-6⟩.

Bauer, C. (1975). Recent studies on transport of respiratory gases by the red blood cell. *Proceedings of the Royal Society of Medicine*, *68*(4), 266–267.

Bryant, S. J., & Anseth, K. S. (2003). Controlling the spatial distribution of ECM components in degradable PEG hydrogels for tissue engineering cartilage. *Journal of Biomedical Materials Research A*, *64*(1), 70–79. http://dx.doi.org/10.1002/jbm.a.10319

Chan, B. P., & Leong, K. W. (2008). Scaffolding in tissue engineering: General approaches and tissue-specific considerations. *European Spine Journal*, *17*(Suppl. 4), 467–479. http://dx.doi.org/10.1007/s00586-008-0745-3

Cohen, S., Yoshioka, T., Lucarelli, M., Hwang, L. H., & Langer, R. (1991). Controlled delivery systems for proteins based on poly(lactic/glycolic acid) microspheres. *Pharmaceutical Research*, *8*(6), 713–720.

Colton, C. K. (1995). Implantable biohybrid artificial organs. *Cell Transplantation*, *4*(4), 415–436.

Cox, T. R., & Erler, J. T. (2011). Remodeling and homeostasis of the extracellular matrix: Implications for fibrotic diseases and cancer. *Disease Models & Mechanisms*, *4*(2), 165–178. http://dx.doi.org/10.1242/dmm.004077

Dahlin, R. L., Kasper, F. K., & Mikos, A. G. (2011). Polymeric nanofibers in tissue engineering. *Tissue Engineering, B: Reviews*, *17*(5), 349–364. http://dx.doi.org/10.1089/ten.TEB.2011.0238

Munoz-Pinto, Dany J., Hou, Yaping, Grunlan, Melissa A., Hahn, Mariah S., & Schoener, Cody. (2010). PDMSstar-PEG hydrogels for directed mesenchymal stem cell differentiation. *Polymer Preprints*, *51*(2), 76.

Drury, J. L., & Mooney, D. J. (2003). Hydrogels for tissue engineering: Scaffold design variables and applications. *Biomaterials*, *24*(24), 4337–4351.

Elbert, D. L. (2011). Liquid-liquid two-phase systems for the production of porous hydrogels and hydrogel microspheres for biomedical applications:

A tutorial review. *Acta Biomaterialia*, *7*(1), 31–56. http://dx.doi.org/10.1016/j.actbio.2010.07.028

Fidkowski, C., Kaazempur-Mofrad, M. R., Borenstein, J., Vacanti, J. P., Langer, R., & Wang, Y. (2005). Endothelialized microvasculature based on a biodegradable elastomer. *Tissue Engineering*, *11*(1–2), 302–309. http://dx.doi.org/10.1089/ten.2005.11.302

Gerecht, S., Townsend, S. A., Pressler, H., Zhu, H., Nijst, C. L. E., Bruggeman, J. P., & Langer, R. (2007). A porous photocurable elastomer for cell encapsulation and culture. *Biomaterials*, *28*(32), 4826–4835. http://dx.doi.org/10.1016/j.biomaterials.2007.07.039

Gnanaprakasam Thankam, F., & Muthu, J. (2013a). Biosynthetic hydrogels-studies on chemical and physical characteristics on long-term cellular response for tissue engineering: Biosynthetic hydrogels. *Journal of Biomedical Materials Research A*, http://dx.doi.org/10.1002/jbm.a.34895, n/a–n/a

Gnanaprakasam Thankam, F., & Muthu, J. (2013b). Influence of plasma protein–hydrogel interaction moderated by absorption of water on long-term cell viability in amphiphilic biosynthetic hydrogels. *RSC Advances*, *3*(46), 24509. http://dx.doi.org/10.1039/c3ra43710h

Gnanaprakasam Thankam, F., Muthu, J., Sankar, V., & Kozhiparambil Gopal, R. (2013). Growth and survival of cells in biosynthetic poly vinyl alcohol–alginate IPN hydrogels for cardiac applications. *Colloids and Surfaces B: Biointerfaces*, *107*, 137–145. http://dx.doi.org/10.1016/j.colsurfb.2013.01.069

Guo, Z., Liu, X.-M., Ma, L., Li, J., Zhang, H., Gao, Y.-P., & Yuan, Y. (2013). Effects of particle morphology, pore size and surface coating of mesoporous silica on Naproxen dissolution rate enhancement. *Colloids and Surfaces B: Biointerfaces*, *101*, 228–235. http://dx.doi.org/10.1016/j.colsurfb.2012.06.026

Helena Janik, I. G. (2010). Synthetic polymer hydrogels for biomedical applications. *Chemistry & Chemical Technology*, *4*(4), 297–305.

Higuchi, A., Komiyama, J., & Iijima, T. (1984). The states of water in gel cellophane membranes. *Polymer Bulletin*, *11*(2), 203–208. http://dx.doi.org/10.1007/BF00258031

Ho, M.-H., Kuo, P.-Y., Hsieh, H.-J., Hsien, T.-Y., Hou, L.-T., Lai, J.-Y., & Wang, D.-M. (2004). Preparation of porous scaffolds by using freeze-extraction and freeze-gelation methods. *Biomaterials*, *25*(1), 129–138.

Huang, G., Wang, L., Wang, S., Han, Y., Wu, J., Zhang, Q., & Lu, T. J. (2012). Engineering three-dimensional cell mechanical microenvironment with hydrogels. *Biofabrication*, *4*(4), 042001. http://dx.doi.org/10.1088/1758-5082/4/4/042001

Muthu, J., Shalumon, K. T., & Mitha, M. K. (2009). Injectable biomaterials for minimally invasive orthopedic treatments. *Journal of Materials Science: Materials in Medicine*, *20*(6), 1379–1387. http://dx.doi.org/10.1007/s10856-008-3683-z

Barry, J. J. A., Rose, F. R. A. J., Buttery, L. D., Hall, I., Shakesheff, K. M., & Barry, J. J. A. (2005). Designing flexible biodegradable scaffolds for cardiac tissue engineering. *European Cells and Materials*, *10*(2), 49.

Khademhosseini, A., & Langer, R. (2007). Microengineered hydrogels for tissue engineering. *Biomaterials*, *28*(34), 5087–5092. http://dx.doi.org/10.1016/j.biomaterials.2007.07.021

Kock, L., van Donkelaar, C. C., & Ito, K. (2012). Tissue engineering of functional articular cartilage: The current status. *Cell and Tissue Research*, *347*(3), 613–627. http://dx.doi.org/10.1007/s00441-011-1243-1

Li, Z., & Guan, J. (2011). Hydrogels for cardiac tissue engineering. *Polymers*, *3*(2), 740–761. http://dx.doi.org/10.3390/polym3020740

Lien, S.-M., Ko, L.-Y., & Huang, T.-J. (2009). Effect of pore size on ECM secretion and cell growth in gelatin scaffold for articular cartilage tissue engineering. *Acta Biomaterialia*, *5*(2), 670–679. http://dx.doi.org/10.1016/j.actbio.2008.09.020

Ma, Z., Mao, Z., & Gao, C. (2007). Surface modification and property analysis of biomedical polymers used for tissue engineering. *Colloids and Surfaces B: Biointerfaces*, *60*(2), 137–157. http://dx.doi.org/10.1016/j.colsurfb.2007.06.019

Mandal, B. B., & Kundu, S. C. (2009). Cell proliferation and migration in silk fibroin 3D scaffolds. *Biomaterials*, *30*(15), 2956–2965. http://dx.doi.org/10.1016/j.biomaterials.2009.02.006

Marques, A. P., Reis, R. L., & Hunt, J. A. (2002). The biocompatibility of novel starch-based polymers and composites: In vitro studies. *Biomaterials*, *23*(6), 1471–1478.

Mitha, M. K., & Muthu, J. (2009). Studies on biodegradable and crosslinkable poly(castor oil fumarate)/poly(propylene fumarate) composite adhesive as a potential injectable biomaterial. *Journal of Materials Science: Materials in Medicine*, *20*(Suppl. 1), S203–S211. http://dx.doi.org/10.1007/s10856-008-3518-y

Provenzano, P. P., Inman, D. R., Eliceiri, K. W., Trier, S. M., & Keely, P. J. (2008). Contact guidance mediated three-dimensional cell migration is regulated by Rho/ROCK-dependent matrix reorganization. *Biophysical Journal*, *95*(11), 5374–5384. http://dx.doi.org/10.1529/biophysj.108.133116

Quirk, R. A., France, R. M., Shakesheff, K. M., & Howdle, S. M. (2004). Supercritical fluid technologies and tissue engineering scaffolds. *Current Opinion in Solid State and Materials Science*, *8*(3–4), 313–321. http://dx.doi.org/10.1016/j.cossms.2003.12.004

Rao, Z., Sasaki, M., & Taguchi, T. (2013). Development of amphiphilic, enzymatically-degradable PEG-peptide conjugate as cell crosslinker for spheroid formation. *Colloids and Surfaces B: Biointerfaces*, *101*, 223–227. http://dx.doi.org/10.1016/j.colsurfb.2012.06.033

Schulte, V. A., Alves, D. F., Dalton, P. P., Moeller, M., Lensen, M. C., & Mela, P. (2013). Microengineered PEG hydrogels: 3D scaffolds for guided cell growth. *Macromolecular Bioscience*, *13*(5), 562–572. http://dx.doi.org/10.1002/mabi.201200376

Shoichet, M. S. (2010). Polymer scaffolds for biomaterials applications. *Macromolecules*, *43*(2), 581–591. http://dx.doi.org/10.1021/ma901530r

Stock, U. A., Wiederschain, D., Kilroy, S. M., Shum-Tim, D., Khalil, P. N., Vacanti, J. P., & Moses, M. A. (2001). Dynamics of extracellular matrix production and turnover in tissue engineered cardiovascular structures. *Journal of Cellular Biochemistry*, *81*(2), 220–228.

Thomson, R. C., Wake, M. C., Yaszemski, M. J., & Mikos, A. G. (1995). Biodegradable polymer scaffolds to regenerate organs. In P. N. A. Peppas, & P. R. S. Langer (Eds.), *Biopolymers II* (pp. 245–274). Berlin Heidelberg: Springer. Retrieved from ⟨http://link.springer.com/chapter/10.1007/3540587888_18⟩.

Vandrovcová, M., Douglas, T., Hauk, D., Grössner-Schreiber, B., Wiltfang, J., Bačáková, L., & Warnke, P. H. (2011). Influence of collagen and chondroitin sulfate (CS) coatings on poly-(lactide-*co*-glycolide) (PLGA) on MG 63 osteoblast-like cells. *Physiological Research/Academia Scientiarum Bohemoslovaca*, *60*(5), 797–813.

Whang, K., Healy, K. E., Elenz, D. R., Nam, E. K., Tsai, D. C., Thomas, C. H., & Sprague, S. M. (1999). Engineering bone regeneration with bioabsorbable scaffolds with novel microarchitecture. *Tissue Engineering*, *5*(1), 35–51.

Xiang, Y.-Q., Zhang, Y., & Chen, D.-J. (2006). Novel dually responsive hydrogel with rapid deswelling rate. *Polymer International*, *55*(12), 1407–1412. http://dx.doi.org/10.1002/pi.2091

Yang, S., Leong, K. F., Du, Z., & Chua, C. K. (2001). The design of scaffolds for use in tissue engineering. Part I. Traditional factors. *Tissue Engineering*, *7*(6), 679–689. http://dx.doi.org/10.1089/107632701753337645

Yokoyama, H., Danjo, T., Ogawa, K., & Wakabayashi, H. (1997). A vital staining technique with fluorescein diacetate (FDA) and propidium iodide (PI) for the determination of viability of myxosporean and actinosporean spores. *Journal of Fish Diseases*, *20*(4), 281–286. http://dx.doi.org/10.1046/j.1365-2761.1997.00293.x

Zeltinger, J., Sherwood, J. K., Graham, D. A., Müeller, R., & Griffith, L. G. (2001). Effect of pore size and void fraction on cellular adhesion, proliferation, and matrix deposition. *Tissue Engineering*, *7*(5), 557–572. http://dx.doi.org/10.1089/107632701753213183

Zhou, C., & Wu, Q. (2011). A novel polyacrylamide nanocomposite hydrogel reinforced with natural chitosan nanofibers. *Colloids and Surfaces B: Biointerfaces*, *84*(1), 155–162. http://dx.doi.org/10.1016/j.colsurfb.2010.12.030